Journal of Sol-Gel Science and Technology (2022) 104:449–455
https://doi.org/10.1007/s10971-022-05876-z

INVITED PAPER: CHARACTERIZATION METHODS OF SOL-GEL AND HYBRID MATERIALS

Hydrogen adsorption and electronic structural calculation of a polymer-derived SiCH membrane with a unique affinity for molecular hydrogen

Yusuke Daiko[1] · Yuji Iwamoto[1]

Received: 12 March 2022 / Accepted: 7 June 2022 / Published online: 6 July 2022

Abstract

In order to understand the hydrogen affinity of polymer-derived SiCH membranes, the amount of adsorbed hydrogen molecules was measured near room temperature, and the stabilization energy for hydrogen adsorption was also calculated by first-principles calculations using the MP2 method. The energies of the highest occupied molecular orbital (HOMO) and the lowest unoccupied molecular orbital (LUMO), the dipole moment of model molecules as well as the charge of the molecular hydrogen, and those relations to the hydrogen molecule affinity were investigated. A linear relationship was found between LUMO energy values and the minimum stabilization energy. It is suggested that a hydrocarbon ring (pore entrance) less than 1 nm on the surface of the SiCH membrane is important as an adsorption site of a hydrogen molecule.

Graphical abstract

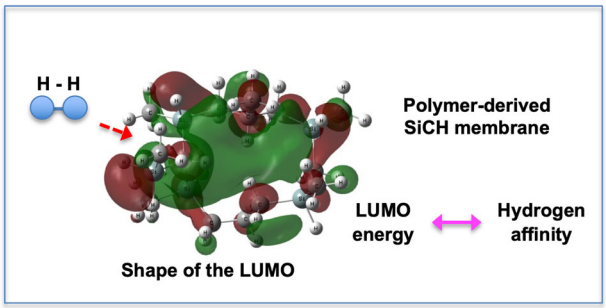

Keywords Solar hydrogen · Hydrogen separation · Hydrogen affinity · Polycarbosilane

Highlights

- The amount of adsorbed hydrogen gas around room temperature on a SiCH membrane was measured by utilizing a quartz crystal microbalance.
- The SiCH membrane adsorbed more molecular hydrogen than helium.
- Calculated LUMO energy values are found to related to the molecular hydrogen affinity.

Supplementary information The online version contains supplementary material available at https://doi.org/10.1007/s10971-022-05876-z.

✉ Yusuke Daiko
daiko.yusuke@nitech.ac.jp

[1] Department of Life Science and Applied Chemistry, Nagoya Institute of Technology, Gokiso-cho, Showa-ku, Nagoya, Aichi 466-8555, Japan

1 Introduction

Hydrogen (H_2) is attracting attention as a clean energy source that does not emit any carbon dioxide or pollutants, and there is a strong need for technological development on how to produce hydrogen effectively and inexpensively [1–3]. In photocatalytic water splitting, electrons at the photocatalyst surface excited to the conduction band by light irradiation reduce water to produce hydrogen, and holes in the valence band oxidize water to produce oxygen. This reaction can proceed near room temperature and is an essentially clean hydrogen production process that does not require fossil fuels and does not emit carbon dioxide [4–6]. However, the fact that the gas produced is a mixture of oxygen and water vapor is a serious issue in photocatalytic water splitting. Because of the risk of explosive combustion of hydrogen with oxygen in a wide range of concentrations from 4 to 94 vol.%, these two gases need to be separated quickly and efficiently near room temperature. In addition, when microporous membranes are used for hydrogen gas separation, water molecules fill the pores of membranes and the separation performance decreases significantly.

We have studied the hydrogen separation properties of various polymer-derived organic-inorganic hybrid membranes around room temperature and under humidified conditions [7–9]. Hybridization of organic components with inorganic SiO_2 network effectively enhances hydrophobicity. Furthermore, in the case of a polycarbosilane (PCS)-based SiCH membrane, it shows high hydrogen gas permeance ($mol \cdot m^{-2} \cdot s^{-1} \cdot Pa^{-1}$) of the 10^{-7} order, and hydrogen permselectivity, $\alpha(H_2/N_2)$, calculated from the ratio of H_2 and N_2 gas permeances reached over 30 even under saturated humidity at 50 °C [8]. Here, materials composed of Si-C, hydrocarbon and Si-H bonds, such as polycarbosilane, are referred to as SiCH (membrane). Note that the kinetic molecular diameter of molecular hydrogen (H_2) is 0.289 nm, which is larger than that of helium (He, 0.26 nm) [10]. Nevertheless, hydrogen gas permeance was higher than He permeance at all the temperatures ranging from 25 to 80 °C, and the apparent activation energy for the hydrogen permeation through the hybrid membrane at 25–80 °C was 17 kJ/mol, which was smaller than that for the He permeation (20 kJ/mol) [8]. In addition, further study on the gas permeations through the SiCH membranes revealed that the observed preferential hydrogen permeation was governed by the solid-state diffusion mechanism [9]. These results suggest that, compared to microporous inorganic membranes such as silica, the hybridization of organic hydrocarbon components improves both the hydrophobicity and the affinity for molecular hydrogen. However, still the origin for the affinity between molecular hydrogen and organic-inorganic hybrid membranes is not well-understood.

In this paper, in order to clarify the change in hydrogen affinity of the hybrid membrane due to the hybridization of organic hydrocarbon components, two studies were carried out: (1) measurement of hydrogen gas adsorption on the hybrid thin film and (2) calculation of hydrogen adsorption energy. A detailed analysis of hydrogen adsorption near room temperature (30–50 °C) was attempted for our previously reported method using a quartz crystal microbalance [8]. Also, the relationships between the molecular parameters (including orbital energies (HOMO, LUMO), total energy, dipole moments) and the stabilization energy when hydrogen gas approaches are discussed by first-principles calculations using a second-order Møller-Plesset (MP2) method [11, 12], which takes into account the electron correlation, in order to clarify the change in the molecular hydrogen affinity of the SiCH membrane. The MP2 method has also been used to calculate molecular hydrogen adsorption on zeolites [13]. Here, benzene, which has a symmetric planar structure, was adopted as a model molecule, and the stability energies were calculated when the H_2 molecule was gradually brought closer to benzene. In the case of planar molecules, the distance to hydrogen molecules is easy to define. The same calculations were also performed for Cl (chlorobenzene) and N (pyridine) substitutions or for increasing the number of rings (anthracene) in order to vary the aforementioned molecular parameters. The hydrogen affinities of silica and a polymer-derived SiCH membrane are discussed based on these computational results.

2 Experimental

2.1 Measurement of hydrogen gas adsorption

The amount of adsorbed hydrogen molecule for the hybrid membrane was measured using a quartz crystal microbalance (QCM). The QCM electrode and an oscillation circuit were purchased from Tamadevice Co., Ltd (Kawasaki, Japan). Commercially available allyl-hydropolycarbosilane (AHPSC) [14, 15] (SMP-10, Starfire Systems, Inc., NY, USA) was diluted 100 times using xylene, dip-coated on QCM electrodes, and then heated at 300 °C under flowing argon (Ar) gas [8]. An oscillation circuit and a QCM electrode were set in a separable flask and heated to a predetermined temperature by a heater (Fig. 1). A thermocouple for heater control was placed right next to the QCM electrode. After reaching a constant oscillation frequency by running He gas for a period of time, hydrogen gas was introduced into the flask. The gas flow rate was set at 30 mL/min. The QCM frequency was recorded using an Iwatsu SC-7205A frequency counter. Conversion from the measured frequency shift Δf [Hz] to the weight change Δm

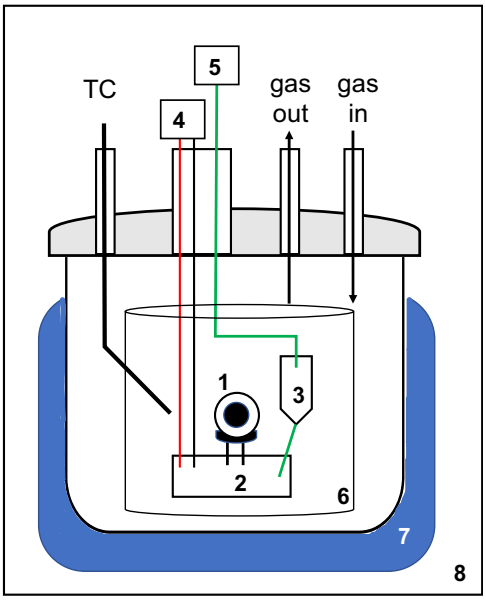

Fig. 1 Schematic illustration of the QCM measurement (1: QCM electrode, 2: oscillator, 3: probe for frequency counter, 4: power supply for the oscillator, 5: frequency counter, 6: aluminum plate, 7: heater, 8: insulated container, TC: thermocouple)

[g] was calculated using the Sauerbrey equation [16];

$$\Delta f = -\frac{2f_0^2}{\sqrt{\mu_q \rho_q}} \frac{\Delta m}{A} \quad (1)$$

where, f_0 is the frequency of the quartz crystal prior to a weight change ($\approx 9.0 \times 10^6$ [Hz]), μ_q is the shear modulus of quartz (2.947×10^{13} [g m^{-1} s^{-2}]), μ_q is the density of quartz (2.648 [g cm^{-3}]), and A is the electrode area (3.93×10^{-5} [m^2]). These constants should change slightly when the temperature is raised from room temperature to 50 °C, however, in this study, temperature changes of these constants are ignored. The measurement system was controlled by a standard PC with a software (Labview, National Instruments Corp., TX, USA) for recording the transition of the frequencies corresponding to the weight change.

2.2 Calculation of stabilization energy

We chose six symmetric molecules with planar structures, and a single point energy calculation at MP2/cc-pVTZ level of theory was performed using Gaussian09 software. Benzene, 1-chlorobenzene, ortho-dichlorobenzene, para-dichlorobenzene, anthracene, and pyridine were adopted as planar target molecules. The total energy (E_{MP2}), the energies of the highest occupied molecular orbital (HOMO) and the lowest unoccupied molecular orbital (LUMO), the dipole moment, and the charge of H_2 molecule were calculated when the H_2 molecule was approached to those planar molecules. Here, if hydrogen atoms are named as H_1-H_2, the calculated charge of H_1 and H_2 atoms was different very slightly, so the average of the charge for two hydrogen atoms was used. In the case of benzene, the stabilization energy S was estimated from the following equation;

$$S = E_{MP2}(Benzene + H_2) - \{E_{MP2}(benzene) + E_{MP2}(H_2)\} \quad (2)$$

where E_{MP2}(benzene) and E_{MP2}(H_2) are the E_{MP2} for benzene and molecular hydrogen only, respectively. The distance between hydrogen atoms was fixed at 0.734 Å, and the two hydrogen atoms were placed on the same plane (same z value).

2.3 Calculation of HOMO and LUMO energies of SiCH network

$Si_5C_{14}H_{38}$ (total 57 atoms) was used to mimic the SiCH network, and structural optimization as well as the calculation of HOMO and LUMO energies were performed using Gaussian09 software (RB3LYP/6-31 G(d)). In addition, a model of SiO_2 shown in Fig. S1 was used and same optimization and calculations were performed.

3 Result and discussion

3.1 Measurement of hydrogen gas adsorption

The hydrogen affinity for a SiCH membrane was investigated by studying the temperature dependence of hydrogen gas adsorption. A quartz crystal microbalance (QCM) can detect a weight change with an accuracy of 1 ng, however its frequency is greatly affected by ambient temperature and electromagnetic noise. As a result, the error in the weight calculated from the vibration frequency is so large that cannot be ignored. The weight change calculated from Eq. (1) for the QCM electrode without the SiCH membrane, with exposure time to He, are shown in Fig. 2. The standard deviation (σ) of the weight versus time for 10 ks is also shown in the figure. The deviation of the weight was very large for a bare QCM electrode (Fig. 2a), probably due to the influence of the heater and surrounding electrical noise, while the noise was reduced significantly by shielding the area around the QCM electrode and oscillation circuit with an aluminum plate (Fig. 2b). Still, the calculated weight changed significantly to follow the temperature change even a temperature fluctuation of only ± 0.5 °C (although the He gas is not being absorbed or desorbed). By optimizing the PID parameters of the heater and keeping the temperature as a constant as possible (± 0.05 °C), the weight was estimated with an accuracy of ± 0.2 ng (Fig. 2c). Because of the

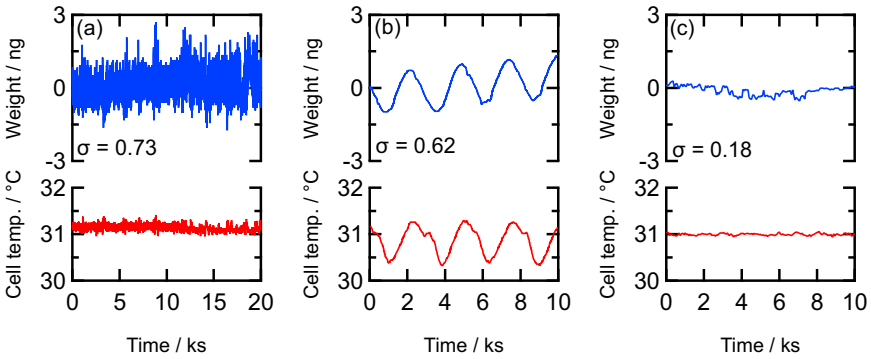

Fig. 2 Changes in temperature and weight with time calculated from the frequency of the QCM electrode (blank) using Eq. 1; **a** Bare QCM electrode, **b** Electrode and oscillation circuit covered with aluminum plate, **c** After optimizing PID parameters of the heater to keep temperature change below ± 0.05 °C

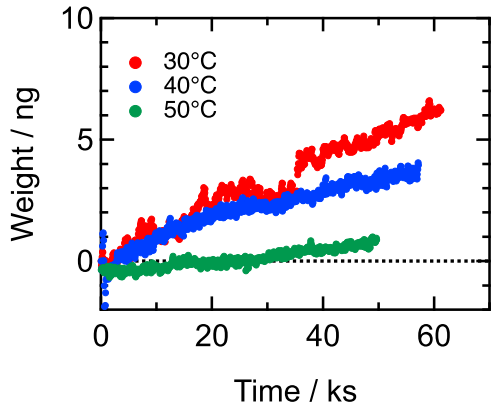

Fig. 3 Changes in weight after exposing to H_2 gas at 30, 40 and 50 °C for the SiCH membrane. Newly prepared films were used for each measurement

extremely light weight of helium and hydrogen, such strict temperature control is indispensable for the measurement of hydrogen adsorption by utilizing QCM.

Figure 3 shows the weight change of the SiCH membrane at each temperature, where helium gas was initially flowed and reached a certain equilibrium frequency before switching to hydrogen gas. Note the weight gain due to the adsorption of hydrogen gas on the SiCH membrane for all the temperatures. Since the molecular weight of H_2 is about one-half that of He, the increase in the weight of the membrane under H_2 atmosphere strongly suggesting the H_2 affinity of the SiCH membrane. At all temperatures ranging from 30 to 50 °C, the amount of adsorbed hydrogen increased almost linearly with exposure time and decreased significantly when the temperature was increased from 30 to 50 °C, which showing typical physisorption characteristics. By utilizing a QCM, temperature dependence of hydrogen gas adsorption on SiCH membrane was clearly measured for the first time.

3.2 Stabilization energy

Six planar molecules were taken as target molecules and the relationship between the electronic state of the molecules and hydrogen (H_2) affinity was investigated. The MP2/cc-pVTZ level includes electron correlation to the second order including London dispersion forces important to the interactions of gas molecules and organic models. Each planar molecule is set at z = 0 as shown in Fig. 4, and these calculations were performed for the distance between the hydrogen and each target molecule from 7.5 Å down to 2.3 Å at 0.05 Å intervals. The calculated stabilization energies of the approaching molecular hydrogen are shown in Fig. 5. The energy minimum is observed around 3 Å, and the larger the negative value, the stronger the interaction between the planar molecule and hydrogen. As shown in Fig. 5a, when hydrogen of the benzene ring is substituted with chlorine, the stabilization energy tends to increase negatively as the number of chlorine substitutions increases in the order benzene - chlorobenzene – dichlorobenzene. In the case of pyridine, the energy curve did not change significantly from that of benzene. On the other hand, in the case of anthracene, the stabilization energy was significantly more negative than that of the other molecules (Fig. 5b). It was also found that none of the molecules interacted with the hydrogen molecule at distances of longer than about 6 Å.

It is considered that the more negative the minimum value of stabilization energy, the stronger the interaction between the hydrogen and the planar molecules. The minimum stabilization energy (S_{min}) for each molecule were obtained from Fig. 5. The dipole moments, HOMO and LUMO energies, HOMO-LUMO gap of each planar molecule and those relation to S_{min} are shown in Fig. 6. The relationship between the charge at the S_{min} point of molecular hydrogen and S_{min} is also shown in the same figure. No linear correlation was found between the dipole moment and S_{min}. For the charge vs S_{min} relationship, the result of anthracene deviated very significantly. Focusing on the HOMO, there was a tendency for S_{min} to decrease with increasing HOMO levels. The distance between the planar model and the hydrogen molecules at S_{min}, and its relation to the dipole moment, HOMO, LUMO energies, and HOMO-LUMO gap of the planar molecules are also shown

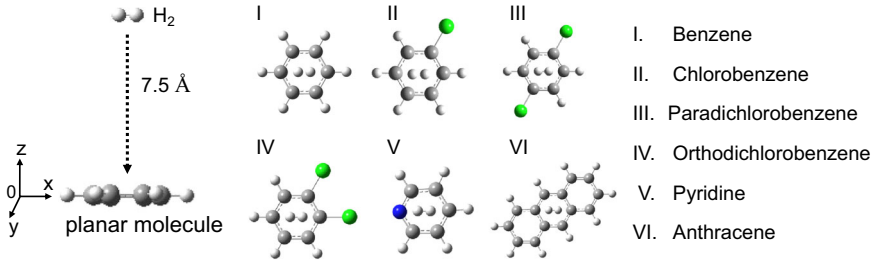

Fig. 4 Structure and configuration of the molecules used in the calculations

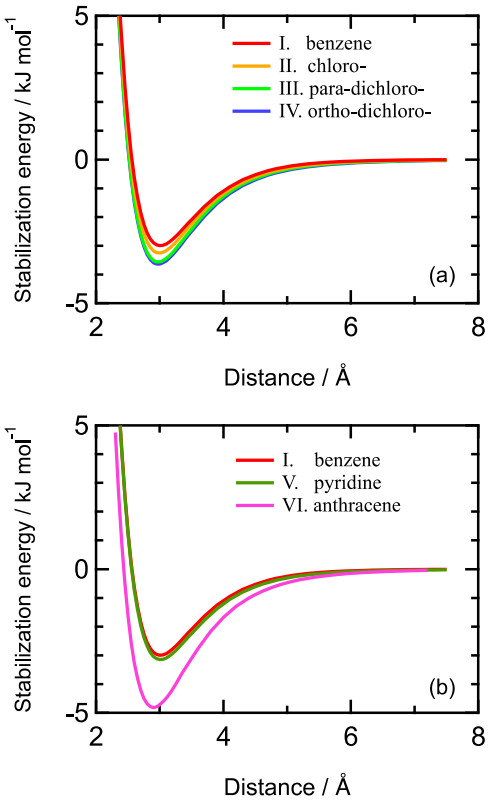

Fig. 5 Change in stabilization energy when a hydrogen molecule is approaching to each planar molecule

in Fig. S2. Note that a very good linear relationship is observed for LUMO energy. For the benzene molecule, the shape of the LUMO at S_{min} is deformed to the side of H_2 molecule in a crown-like shape, supporting that there is a certain interaction between the two molecules (Fig. S3).

We consider this result is related to the reducibility of molecular hydrogen. When the LUMO energy of the target molecule lowers, it is more likely to accept electrons from the outside (= more likely to be reduced). This is related to the fact that a lower LUMO energy attracts more hydrogen molecules. First-principles calculations using these planar molecules show that the LUMO level is strongly related to the S_{min}, and that the lower the LUMO energy value, the stronger the interaction with hydrogen molecules. These relations between the electronic state of molecules and S_{min} should hold regardless of the type of material (organic, inorganic, or hybrid).

3.3 Molecular hydrogen affinity for SiCH membrane

In the case of the planar molecule shown in Fig. 5, the repulsive force increases when the hydrogen gets closer than about 3 Å, and it cannot get any closer. On the other hand, in the SiCH-based H_2 permeable membranes as aforementioned, the existence of micropores less than 1 nanometer has been pointed out [8, 9], and these pores are considered as hydrogen-selective solubility site for preferential permeation through the SiCH network. In the AHPCS precursor, C=C double bonds of the allyl group change to C-C single bonds upon heating above 300 °C (Fig. S4). Then we employed a $Si_5C_{14}H_{38}$ (total 57 atoms) ring comprising only single bonds to mimic the micropores in the SiCH network. A ring structure of less than 1 nanometer was optimized and the result is shown in Fig. 7a. We regarded this ring to be an entrance of a micropore presented on the SiCH membrane surface. Here, the MP2 method is very computationally time-consuming. The relationship between HOMO and LUMO obtained by the MP2 and DFT methods, respectively, is shown in Fig. S5. Although the absolute values were different, a good linear relationship was found between the results obtained with MP2 and DFT methods. Thus, the optimized structure was used to calculate the energy of HOMO and LUMO using RB3LYP/6-31 G(d) basis set instead of MP2 method. The shape of the LUMO is depicted overlaid in Fig. 7b. The HOMO shape is also shown in Fig. S6 for comparison. Note that the LUMO is spread over the interior of the ring shape. Molecular hydrogen is thus expected to be more stable in the ring. The HOMO and LUMO energies of molecular hydrogen, SiO_2 and the SiCH membrane are shown in Fig. 8. The presence of hydrocarbon ($-CH_2-CH_2-CH_2-$ in this case, formed in situ via thermal cross-linking between Si-H and allyl groups) increased the HOMO while decreasing the LUMO energies compared to the silica. As discussed in Fig. 6, both the increase in HOMO and the decrease in LUMO energies are related to the increase in hydrogen affinity.

As mentioned above, the dominant mechanism for the preferential hydrogen gas permeation through the polymer-

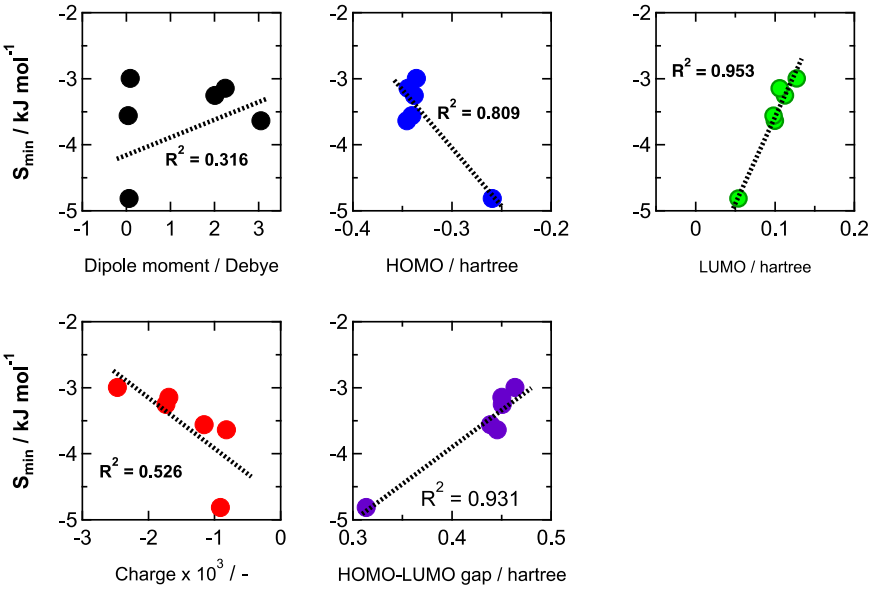

Fig. 6 The minimum stabilization energy (S_{min}) as a function of dipole moment, HOMO, LUMO energies, charge of H_2 molecule and HOMO-LUMO gap of the planar molecules

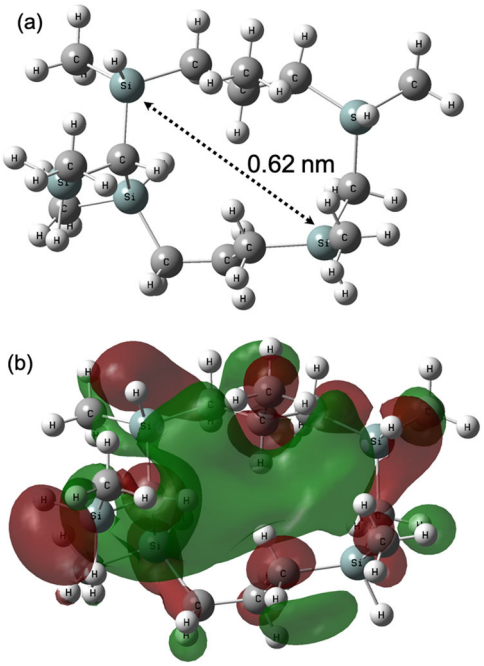

Fig. 7 **a** The optimized SiCH network with $Si_5C_{14}H_{38}$ (total 57) atoms. **b** The shape of the LUMO obtained using RB3LYP/6-31 G(d) basis set

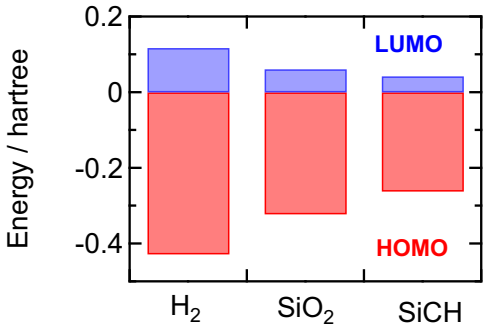

Fig. 8 The energies of HOMO and LUMO of H_2 molecules, SiO_2, and SiCH network shown in Fig. 6. The structure of SiO_2 calculated is shown in Fig. S4)

derived SiCH membranes [8, 9] was suggested as solid-state diffusion mechanism [17], and it involves the solubility of molecular hydrogen and its diffusion in the solid phase. Here, if the SiCH membrane has a connecting pore of approximately 0.62 nm, it is more than twice the size of a hydrogen molecule (0.289 nm), which could reduce hydrogen gas selectivity. Although calculations for various ring sizes are needed, calculation results strongly suggest that the presence of a ring composed of hydrocarbons on the membrane surface facilitates the adsorption of hydrogen into the membrane compared with SiO_2. We conclude that the change in molecular orbital energy due to the introduction of a hydrocarbon group is related to the molecular hydrogen affinity of the SiCH membranes. We are now conducting detailed analyses based on experiments and calculations for more suitable functional group types, pore sizes design for the polymer-derived ternary SiCH and SiOCH (having polymeric backbone containing oxygen) systems.

4 Conclusion

The reason why polymer-derived SiCH membranes show superior selective permeation of hydrogen gas compared to silica membranes is considered based on the measurement of the hydrogen gas adsorption and the calculation result of the molecular orbital. We successfully measured the amount of adsorbed hydrogen gas around room temperature by utilizing a quartz crystal microbalance. The SiCH membrane adsorbed

more molecular hydrogen than helium, while the amount of adsorbed hydrogen decreased significantly when the temperature was increased from 30 °C to 50 °C. A slight interaction (an attraction force) between the SiCH membrane and molecular hydrogen is considered to be working. In addition, using benzenes with various functional groups as model molecules, the relationship between their electronic state and hydrogen affinity was investigated. In particular, LUMO energy values were found to related to molecular hydrogen affinity, and the LUMO energy is lower for the SiCH than that for SiO_2. This orbital change relates to the improvement of hydrogen affinity by hybridization of hydrocarbon groups.

Acknowledgements We acknowledge H. Mitsukawa and K. Naniwa for assistance of the calculation and QCM experiment.

Compliance with ethical standards

Conflict of interest The authors declare no competing interests.

Publisher's note Springer Nature remains neutral with regard to jurisdictional claims in published maps and institutional affiliations.

References

1. Huber GW, Iborra S, Corma A (2006) Synthesis of transportation fuels from biomass: Chemistry, catalysts, and engineering. Chem Rev 106:4044–4098
2. Singla S, Shetti NP, Basu S, Mondal K, Aminabhavi TM (2021) Hydrogen production technologies - Membrane based separation, storage and challenges. J Environ Manag 302:113963
3. Andaveh R, Darband GB, Maleki M, Rouhaghdam AS (2022) J Mater Chem A https://doi.org/10.1039/d1ta10519a
4. Maeda K, Domen K (2007) New non-oxide photocatalysts designed for overall water splitting under visible light. J Phys Chem C 111:7851–7861
5. Wang Q, Hisatomi T, Jia Q, Tokudome H, Zhong M, Wang C, Pan Z, Takata T, Nakabayashi M, Shibata N, Li Y, Sharp LD, Kudo A, Yamada T, Domen K (2016) Scalable water splitting on particulate photocatalyst sheets with a solar-to-hydrogen energy conversion efficiency exceeding 1. Nat Mater 15:611–615
6. Goto Y, Hisatomi T, Wang Q, Higashi T, Ishikiriyama K, Maeda T, Sakata Y, Okunaka S, Tokudome H, Katayama M, Akiyama S, Nishiyama H, Inoue Y, Takewaki T, Setoyama T, Mineshige T, Takata T, Yamada T, Domen K (2018) A particulate photocatalyst water-splitting panel for large-scale solar hydrogen generation. Joule 2:509–520
7. Kumo M, Kojima M, Mano R, Daiko Y, Honda S, Iwamoto Y (2020) A hydrostable mesoporous γ-Al2O3 membrane modified with Si–C–H organic-inorganic hybrid derived from polycarbosilane. J Memb Sci 598:117799
8. Kubo M, Mano R, Kojima M, Naniwa K, Daiko Y, Honda S, Ionescu E, Bernard S, Riedel R, Iwamoto Y (2020) Hydrogen selective SiCH Inorganic–Organic Hybrid/γ-Al2O3 composite membranes. Membranes 10:258
9. Kubo M, Okibayashi K, Kojima M, Mano R, Daiko Y, Honda S, Bernard S, Iwamoto Y (2021) Superhydrophobic polycarbosilane membranes for purification of solar hydrogen. Sep Purif Tecnhol 258:117998
10. Briceno K, Garcia-Valls R, Montane D (2010) Asia-Pac. J Chem Eng 5:169–178
11. Møller C, Plesset MS (1934) Note on an approximation treatment for many-electron systems. Phys Rev 46:618–622
12. Kayanuma M, Ikeshoji T, Ogawa H (2011) Theoretical study of hydrogen chemisorption to nitrogen-substituted graphene-like compounds. Bull Chem Soc Jpn 84:52–57
13. Prakash M, Sakhavand N, Shahsavari R (2013) H2, N2, and CH4Gas adsorption in zeolitic imidazolate framework-95 and -100: Ab initio based grand canonical Monte Carlo simulations. J Phys Chem C 117:24407–24416
14. Elyassi B, Deng W, Sahimi M, Tsotsis TT (2013) On the use of porous and nonporous fillers in the fabrication of silicon carbide membranes. Ind Eng Chem Res 52:10269–10275
15. Dabir S, Deng W, Sahimi M, Tsotsis TT (2017) Fabrication of silicon carbide membranes on highly permeable supports. J Memb Sci 537:239–247
16. Sauerbrey G(1959) Zeitschrift für Phys 155:206–222 https://doi.org/10.1007/BF01337937
17. Ahn SJ, Yun G-N, Takagaki A, Kikuchi R, Oyama ST (2018) Synthesis and characterization of hydrogen selective silica membranes prepared by chemical vapor deposition of vinyltriethoxysilane. J Memb Sci 550:1–8